Peer-reviewed version available at Materials 2018, 11, 174; doi:10.3390/ma11020174

Article

Characterization of different cable ferrite materials to reduce the electromagnetic noise in the 2-150 kHz frequency range

Adrian Suarez [1,*], Jorge Victoria [1,2], Antonio Alcarria [1,2], Jose Torres [1], Pedro A. Martinez [1], Julio Martos [1], Jesús Soret [1], Raimundo Garcia-Olcina [1] and Steffen Muetsch [2]

[1] Department of Electronic Engineering, University of Valencia, Burjassot, 46100, Spain
[2] Würth Elektronik eiSos GmbH & Co. KG, Waldenburg, 74638, Germany
* Correspondence: adrian.suarez@uv.es; Tel.: +34-963-544-146

Abstract: The gap of standardization for conducted and field coupled electromagnetic interferences (EMI) in the 2–150 kHz frequency range can lead to Electromagnetic Compatibility (EMC) problems. This is caused by power systems such as PWM controlled rectifiers, photovoltaic inverters or charging battery units in electric vehicles. This is a very important frequency spectral due to interferences generate in a wide range of dives and, specifically, communication problems in the new technologies and devices incorporated to the traditional grid to convert it into Smart Grid. Consequently, it is necessary to provide new solutions to attenuate this kind of interferences, which involve finding new materials able to filter the electromagnetic noise. This contribution is focused on characterizing the performance of different cable ferrite compositions in order to determine the effectiveness of most common materials such as MnZn and NiZn and a new range based on nanocrystalline solutions. This analysis procedure is carried out through two methods: theoretical method by determining the insertion loss through measuring impedance parameter and proposing a new empirical technique based on measuring directly the insertion loss parameter. Therefore, the main aim of this characterization process is to determine the performance of these cable ferrites to reduce the interferences in this controversial frequency range. From the results obtained, it is possible to deduce that nanocrystalline cable ferrites provide the best performance to filter the electromagnetic noise in the 2-150 kHz frequency range.

Keywords: Cable ferrite; electromagnetic interferences; low frequency emissions; nanocrystalline; relative permeability; insertion loss.

1. Introduction

Standardization regarding disturbances in the 2-150 kHz frequency range is progressing in recent years and are classified into the conducted electromagnetic interferences (EMI) range as power quality harmonics (2-9 kHz) and CISPR A band (9-150 kHz) [1,2]. Nevertheless, there is still a gap in the limits standardized that can result in interferences between devices at 2-150 kHz band. Electromagnetic disturbances located from 2 kHz to 150 kHz are known as supraharmonics and they are generated by most mains related to power conversion applications, like battery electrical vehicles chargers [3] or photovoltaic systems [4]. Furthermore, these disturbances have been also detected in other kinds of systems related to household appliances such as washing machines [5] and lighting installations [6].

One of the reasons of this problem is due to the lack of knowledge and controllability of the low voltage harmonic grid impedances and the high sensitivity of devices to generate electromagnetic disturbances. These interferences can be caused by its internal circuit topology or the presence of certain neighbor devices connected to the same grid [7]. An important problem caused by this kind of electromagnetic noise is related to the systems and devices included in the electrical network to

convert it into a Smart Grid [8]. This is a significant area because one of the main consequences of Smart Grid is a strong increase in use of electronics to include the intelligence in the power system. This makes that the correct function of electronic equipment needs to be take into account for implementing a smart power grid, which integrates intelligently, the actions of all users in order to promote renewable energy sources and efficiently use of electricity.

Specifically, most of the smart meters used to determine the power consumption are typically equipped with communication interfaces to transmit the readings to the network operator or Power Company through Power Line Communication (PLC) protocol (9 to 95 kHz). By lacking proper legislation, the frequency band 2-150 kHz has been used as the 'garbage' band during the last years [9], generating as a result, interferences in the PLC communication. Therefore, it has to be guaranteed that the unintentional emissions or interferences are lower than the intentional emission by the PLC in order to ensure its proper functionality in the 2-150 kHz frequency band.

Thereby, it is essential to ensure the electromagnetic compatibility (EMC) in the 2-150 kHz frequency band in terms of radiated and conducted disturbances. Consequently, new solutions in terms of EMI filtering have to be proposed with the aim of reducing the electromagnetic noise, which can cause disturbances in this spectral band. An interesting component that is widely used by designers to meet EMC compliance requirements is the ferrite.

Ferrite is a generic term for a class of nonconductive ceramics that are based on materials such as oxides of iron, cobalt, nickel, zinc or magnesium. Ferrite manufacturers have even designed their own compositions, this implies that there is a large variety of ferrite combinations.

Ferrites provide an inexpensive way of coupling high-frequency resistance into a circuit without introducing power loss at dc or affecting any low-frequency signals present. Traditionally, ferrites have been most effective in providing attenuation of unwanted signals above 1 MHz because these components can provide the suppression of high-frequency oscillations, common-and differential-mode filtering, and the reduction of conducted and radiated emissions [10,11]. The material used to make a ferrite determines the frequency range of applicability. They are available in many different configurations, such as thru-hole beads on leads, surface-mount beads, sleeve cable cores, flat cable cores, snap on cores, toroids, etc. This contribution is focused on analyzing the performance of cable cores or also known as cable ferrites, due to these components slip over a conductor lead and, hence provide a solution against EMI without the need of electronic circuit redesign.

Cable ferrite EMI suppressors are applied widely in electronics and telecommunications since they are able to suppress interference over a wide frequency range. They are generally focused on filtering interferences in the Megahertz band and the most common compositions are MnZn and NiZn variety [12,13]. The used of MnZn cable ferrites is usually limited to higher Kilohertz and very low Megahertz region, whereas ferrite cores made of NiZn material work in a broadband frequency range which can cover several hundreds of Megahertz and even frequencies about 1 GHz.

Some researchers have looked into the use of another material such as nanocrystalline (NC) [14] to make other EMC components, such as the common-mode-choke (CMC) in order to filter interferences. This is due to NC cores provide better insertion losses at low frequencies, the volume of the component can be reduced by 50–80%, high permeability, saturation and inductive behavior near CMC resonance [15]. CMC based on NC cores are important components to reduce the noise spectrum in application such as Switch Mode Power Supply (SMPS) in which the noise spectrum is concentrated in frequencies bellow 200 kHz or inverters where the interferences usually appear from 10 kHz to 30 MHz.

NC is a magnetic material which is being increasingly used in other types of applications where low frequency electromagnetic noise can become a problem, such as energy storage, current sensors or electronic filters [16]. The main advantage of NC material is that due to the materials intrinsic properties it can be used to design more reduced passive components for low frequency applications. Their innate advantages such as medium saturation, low thickness, high resistivity and low magnetic losses, and the ability to design different shapes of hysteresis cycle have motivated various industries to further extending their field of application [17]. This benefit combined with others such as medium saturation, low thickness, high resistivity and low magnetic losses have motivated that the EMC

Peer-reviewed version available at Materials 2018, 11, 174; doi:10.3390/ma11020174

industry focused on developing new filtering products based on NC material. Nevertheless, the main drawback of this material resides in the very complex manufacturing process due to it is brittle. Therefore, this last factor results in an increase of the production costs.

The target of this research is to determine the performance of cable ferrite components based on nanocrystalline material with the aim of studying its suitability for solving or reducing EMC problems in the frequency range of 2-150 kHz. Thereby, a NC core is characterized and compared with MnZn and NiZn cores in order to determine the effectiveness of each material in that controversial frequency range. This is performed by measuring and analyzing their relative permeability and impedance response. In addition, the insertion loss (A) parameter of each cable ferrite is determined in order to know the attenuation ration that a certain cable ferrite can provide in a specific frequency. This parameter is usually estimated by means of the cable ferrite impedance [11], however, this contribution proposes an experimental method, which simulates supraharmonics generated to determine the insertion loss. Therefore, a comparison between the insertion loss parameter calculated from the cable ferrite impedance and the attenuation measured with the experimental setup is carried out.

2. Materials and Methods

2.1 Cable Ferrites Characterization

The most common ferrite geometry used in noise-suppression applications is the cylindrical core. A cable ferrite placed around a cable acts as common-mode choke and it can be effective in reducing both conducted and radiated emission. Thereby, the greater the length of the cylinder, the higher the impedance, so an increase of the core length is equivalent to use several ferrites together. The attenuation provided by a certain cable ferrite depends on the impedance of the system in which this is placed, thus, the cable ferrite should have an impedance higher than the system impedance at the frequency of interest. Hence, they are used most effectively in low-impedance circuits. [10].

An interesting characteristic of cable ferrites is the possibility of rolling around them multiple turns of the cable to be filtered. With this technique, the ferrite impedance can be increased proportional to the number of turns squared. However, there is a balance between number of turns and interwinding capacitance because of the higher the number of turns, the worse the performance at high frequencies. Therefore, the behavior of a cable ferrite can be improved in the 2-150 kHz frequency range, although, should not be overlooked. It is not common to use more than two or three turns.

The impedance of a certain material is defined by its internal characteristics and, in the case of cable ferrites, one of the most important parameters that describes the material's capacity to absorb electromagnetic noise is the permeability (μ). The permeability parameter relates the magnetic flux density to the magnetic field in a defined medium, thus, when a ferromagnetic material such a cable ferrite is placed in a magnetic field, the magnetic flux is concentrated in it. Thereby, the parameter that determines the factor, by which the induction (B) is modified when a material is introduced, is the relative permeability (μ_r) [18]. The losses of the magnetic flux can be quantified by separating it into its complex form so that the real component is related to the reflection or inductive part and the imaginary component provides the losses or absorption part [19,20]. The real part is represented by μ' which defines the magnetic flux that the material is able to reflect and the imaginary part corresponds to μ'' which describes the core material effectiveness to absorb the magnetic noise.

The behavior of these parameters depends on the material internal composition and it is usually represented versus the frequency. One way of knowing the performance of the three different cable ferrites materials mentioned above, is through examining the permeability parameter. Figure 1 represents the relative permeability traces of NC, MnZn and NiZn cable ferrite compositions split into real and imaginary components.

Preprints (www.preprints.org) | NOT PEER-REVIEWED | Posted: 13 December 2017 doi:10.20944/preprints201712.0081.v1

Peer-reviewed version available at Materials 2018, 11, 174; doi:10.3390/ma11020174

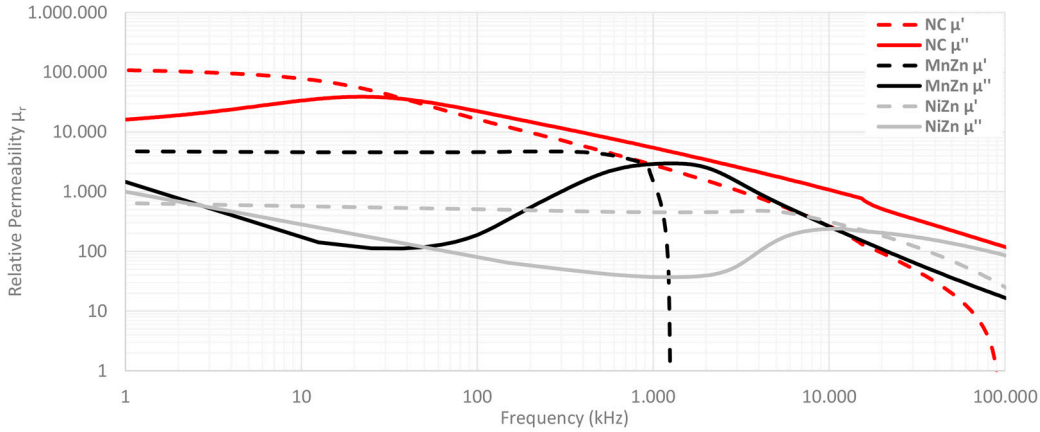

Figure 1. Complex Relative Permeability of NC, MnZn and NiZn cable ferrites compositions.

The relative permeability parameter and impedance of a certain cable ferrite are conditioned by, on the one hand, the imaginary component is related to the loss or resistive component and, on the other hand, the real component corresponds to the inductance component. The mathematical expressions which demonstrate this are given by:

$$\mu' = \frac{\ell L}{\mu_0 N^2 A} \quad (1)$$

$$\mu'' = \frac{\ell R}{\mu_0 N^2 \omega A} \quad (2)$$

where ℓ corresponds to average magnetic path length of toroidal core [m], μ_0 is the permeability of the air, N is the number of turns given with a cable to carry out the measure, A is the cross-sectional area of the toroidal core [m^2], ω is the angular frequency, R is the resistive or loss component and L is the inductance component of the cable ferrite.

Although the permeability is one of the most important parameter which defines the performance of a cable ferrite, other means of characterizing this component is through specifying the magnitude of the impedance versus frequency. The magnitude of the impedance is given by:

$$|Z_F| = \sqrt{R^2 + (X_L)^2}, \quad (3)$$

where R is the equivalent resistance of the cable ferrite and X_L is the impedance of the inductive part. The datasheets of this kind of component generally provides the trace of the ferrite impedance in the frequency range where it is effective or only specify the impedance at several frequency points. The recommended frequency range for various ferrite materials when used in noise suppression applications is shown in Figure 2. As it can be observed, traditional ferrite components such as MnZn and NiZn are available for use over the frequency range of 150 kHz to 1 GHz, whereas NC is intended for covering lower frequencies.

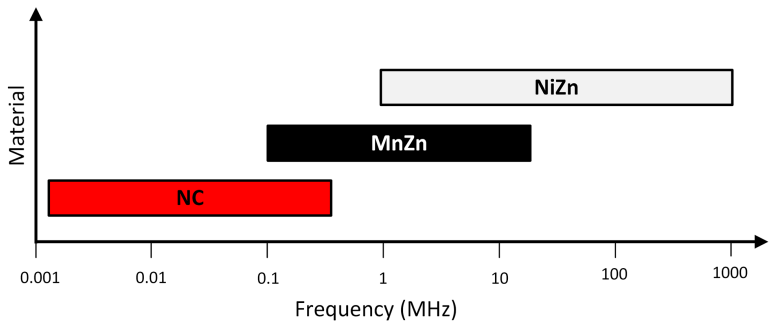

Figure 2. Material composition versus frequency range covered.

Peer-reviewed version available at Materials 2018, 11, 174; doi:10.3390/ma11020174

The cable ferrites that have been characterized in this contribution have been selected because they have similar dimensions and, at the same time, they are composed with different materials. Thereby, it is possible to evaluate their performance to solve electromagnetic noise problems found below 150 kHz. These parameters are shown in Table 1.

Table 1. Lists of cable ferrites used in this contribution.

Ferrite part number	Magnetic material	External diameter (mm)	Internal diameter (mm)	Height (mm)
M-4304-02	NC	18,9	12,9	27,7
74277255	MnZn	18,6	10,2	28,5
74270055	NiZn	18,6	10,2	28,5

2.2 Theoretical Insertion Loss Calculation Method

One of the most common methods used to characterize a cable ferrite is based on measuring its impedance. The impedance of a cable ferrite can be separated into two components. When this EMC component is used to suppress electromagnetic noise, the loss resistance (R), which represents the losses, needs to be taken into account. Figure 3 illustrates the contribution of loss resistance as well as inductance (X_L) to the magnitude of the impedance of the NC cable ferrite analyzed in this research. The parameters plotted on this graph has been measured through carrying out the reflection method with a Vector Network Analyzer (Keysight E5061B) together with the Terminal Adapter 16201A and the Spring Clip Fixture 16092A by rolling one turn in the component [21]. Thereby, it can be observed in Figure 3 how the inductance is stable in a certain frequency range and show strong frequency range dependence above around 10 kHz. Above 30 MHz the inductance falls sharply, down to zero at around 80 MHz. The loss component (R) grows continuously with frequency and reaches the same value as the X_L component at the so-called ferromagnetic resonance frequency. The resistance value rises until MHz range and dominates over the magnitude impedance (Z_F).

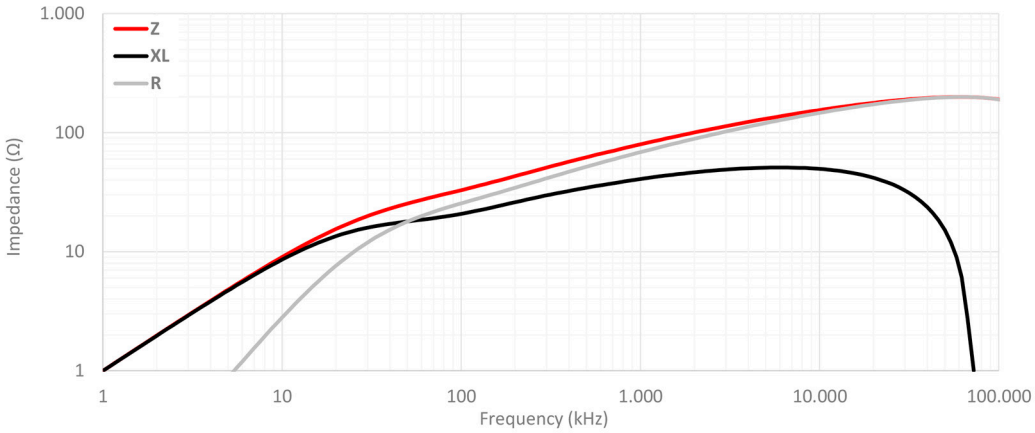

Figure 3. Magnitude of the impedance measured of NC cable ferrite and its components R and X_L.

The attenuation that this kind of component is able to provide in a certain conductor is not usually specified in datasheets in contrast to other EMC products such as common-mode-chokes. This is due to the insertion attenuation or insertion loss (A) that a cable ferrite is able to provide mainly depends on the impedance of the system in which it is placed. Subsequently, the source impedance (Z_A) and the load impedance (Z_B) of the system with electromagnetic interference problems as well as the impedance which the ferrite core introduces in that system (Z_F) are related in order to obtain an approach of the insertion loss parameter [11]. According with this, taking into

Peer-reviewed version available at Materials 2018, 11, 174; doi:10.3390/ma11020174

account the system impedance and the ferrite impedance in a specific frequency value, the insertion loss in terms of decibels can be theoretically calculated by using this equation:

$$A(dB) = 20 \log \frac{Z_A + Z_F + Z_B}{Z_A + Z_B}, \quad (4)$$

The block diagram used to obtain this equation and to analyze the effect of placing a cable ferrite into a certain system is shown in Figure 4.

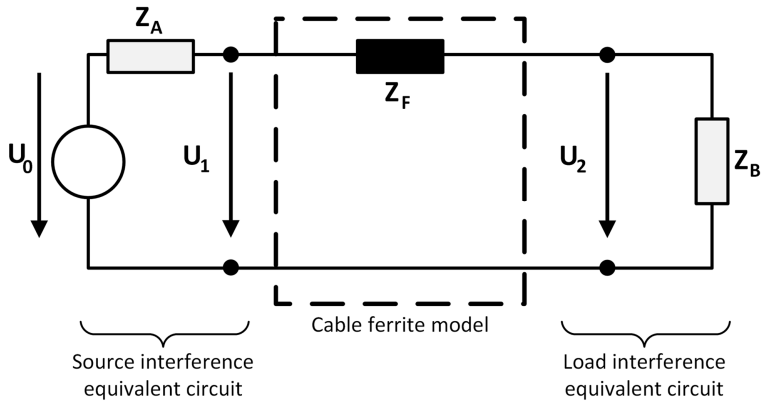

Figure 4. Diagram of source and load equivalents circuits used to determine the insertion loss parameter of a cable ferrite when it is introduced into a system.

2.3 Insertion Loss Experimental Measurement Setup

The setup used to determine the insertion loss of several cable ferrites is focused on simulating the block diagram shown in Figure 4, where the source and load impedance are known and the parameter to study is the impedance of the ferrite core. Thereby, the setup designed to simulate that diagram is shown in Figure 5 and it consists of:

- A low frequency immunity test system based on a Low Frequency Signal Generator (TESEQ NSG-4060/1) with 50 Ω of output impedance is employed to generate the reference signal that crosses the cable ferrite. Thus, this 50 Ω output resistance represents the Z_A in the insertions loss block diagram. This sine wave generator and integrated power amplifier consists of a signal generator able to provide signals for the frequency range of 15 Hz to 150 kHz. The probe connected to this generator separates the signal and the ground terminals to place the cable ferrite only in the signal path. The main objective of this part of the setup is focused on characterizing the performance of cable ferrites in this range of frequencies through simulating the electromagnetic noise which can appear in a real system.
- A Spectrum Analyzer (Keysight N9010A) is used both measuring the amplitude of the signal generated as a reference and the signal when the cable ferrite is placed around the cable. This equipment makes it possible to analyze the attenuation provided by each kind of cable ferrite in the range of 2-150 kHz. The measurement is carried out with a low frequency current probe which measures the signal before and after placing the cable ferrite.
- Different resistance loads are employed to evaluate the performance and robustness of ferrites. In order to analyze the characteristics of cable ferrites with different values of load impedance, a PCB (Printed Circuit Board) which holds several values of impedance have been designed. This circuit is intended for switching among four different values of Z_B 5 Ω, 50 Ω, 100 Ω and 1000 Ω. Since the performance of cable ferrites relies on the load impedance, this part of the setup allows studying the behavior of each material composition in systems with different load values.

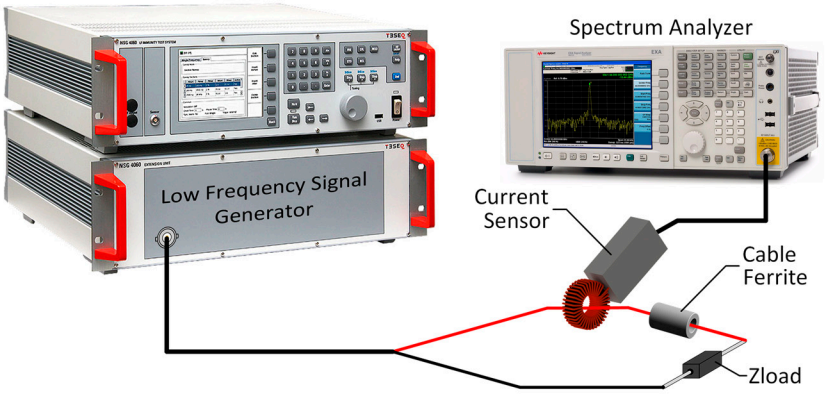

Figure 5. Measurement setup diagram to characterize cable ferrites in the 2-150 kHz frequency range.

Therefore, the test is carried out by attaching the current probe in the signal terminal of the signal generator probe and measuring the noise emitted with the Spectrum Analyzer. This is tuned to measure the interference signal generated by the Low Frequency Signal Generator in the 2-150 kHz band. This measurement process is repeated twice: only measuring the signal terminal, and measuring with the cable ferrite placed around the signal terminal.

Subsequently, both signals stored will be compared and the attenuation rate or insertion loss parameter of a certain cable ferrite can be determined by subtracting the reference signal with the signal measured after attaching the EMC component. Both measurements are acquired with the max-hold option enabled in the Spectrum Analyzer in order to compare them.

3. Results and Discussion

The results presented in this part, correspond to the analysis of the acquired data through the theoretical and experimental methods described above. Firstly, the insertion loss parameter of the three cable ferrites under test has been calculated accordingly with the described theoretical method. Subsequently, the insertion loss parameter measured by following the experimental setup explained are plotted in order to compare both methods and characterize the three cable ferrites at low frequency range. Considering this, it is possible to evaluate the performance of nanocrystalline cable ferrite to provide a solution to filter the electromagnetic noise in the 2-150 kHz spectrum range and compare it with the another materials analyzed.

3.1 Theoretical Insertion Loss Results

As it has been described in 2.2 section, theoretical insertion loss parameter is calculated from the magnitude of the impedance. This graph makes visible that the impedance of NC cable ferrite is higher than MnZn and NiZn components until 700 kHz. From this frequency, MnZn cable ferrite provides a greater performance, although its initial magnitude impedance is lower, the angle of slope of its trace is higher than NC. With regard to NiZn cable ferrite trace, it can be observed how its impedance is much lower if this is compared with NC and MnZn materials because it is destined to higher frequency range.

Peer-reviewed version available at Materials 2018, 11, 174; doi:10.3390/ma11020174

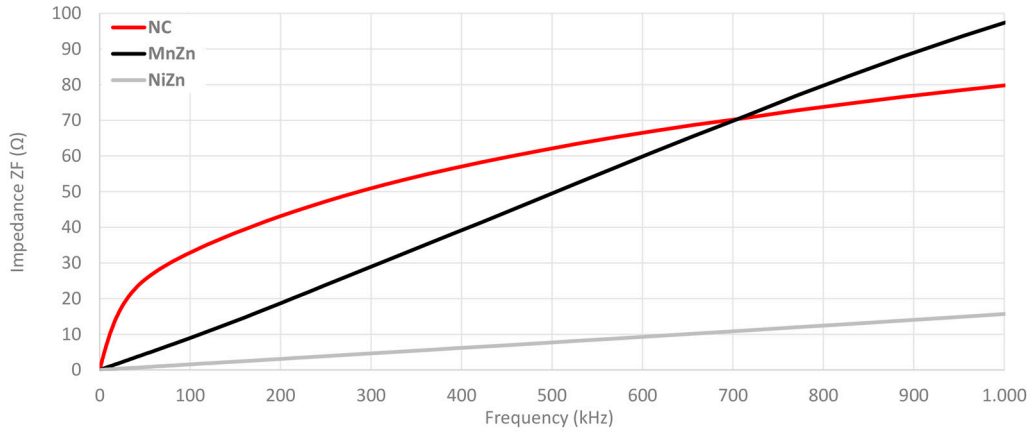

Figure 6. Impedance comparison of the three cable ferrites measured with 1 turn.

This measurement has been repeated, but in this case, by using two turns as shown in Figure 7. This change generates higher values of magnitude impedance in the three traces and a shift in the cross point of NC and MnZn traces. Thereby, if 100 kHz point is taken as a reference, three traces has been increased about four times (the number of turns squared). Specifically, in the case of NC from 33.2 Ω to 132.7 Ω, MnZn 9.2 Ω to 36.6 Ω and NiZn cable ferrite from 1.6 Ω to 5.0 Ω. As regards the cross point between NC and MnZn traces, it has been moved from 705 kHz to 680 kHz when two turns are winded in the cable ferrites.

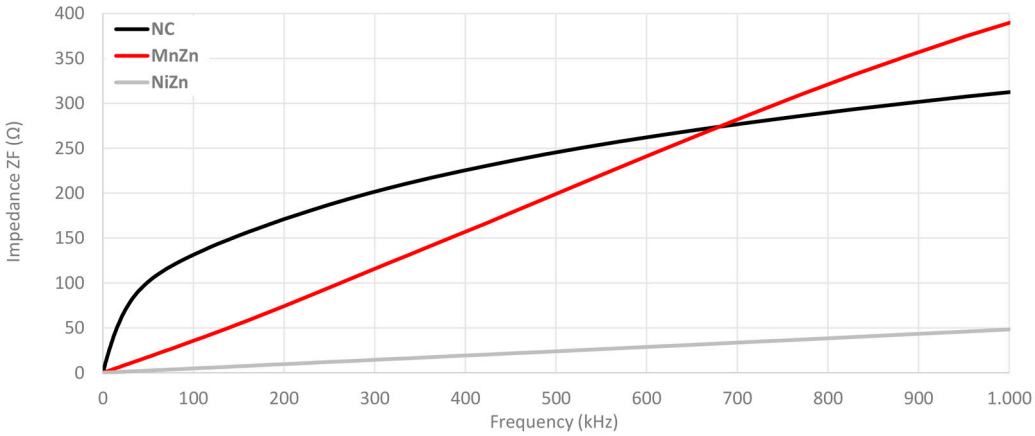

Figure 7. Impedance comparison of the three cable ferrites measured with 2 turns.

A zoom in on 2-150 kHz frequency range is performed as shown in Figure 8 in order to analyze in detail the impedance provided for each cable ferrite when one and two turns are winded. This graph demonstrates the huge difference among the impedance provided by NC cable ferrite and the others. If 100 kHz is taken as a reference, NC provides 24.0 Ω more than MnZn and 31.6 Ω than NiZn cable ferrites with one turn. Considering two turns, NC impedance is 96.1 Ω higher than MnZn and 127.7 Ω. It can be also observed that NC with one turn is even higher than MnZn with two turns until 88 kHz.

Preprints (www.preprints.org) | NOT PEER-REVIEWED | Posted: 13 December 2017 doi:10.20944/preprints201712.0081.v1

Peer-reviewed version available at Materials 2018, 11, 174; doi:10.3390/ma11020174

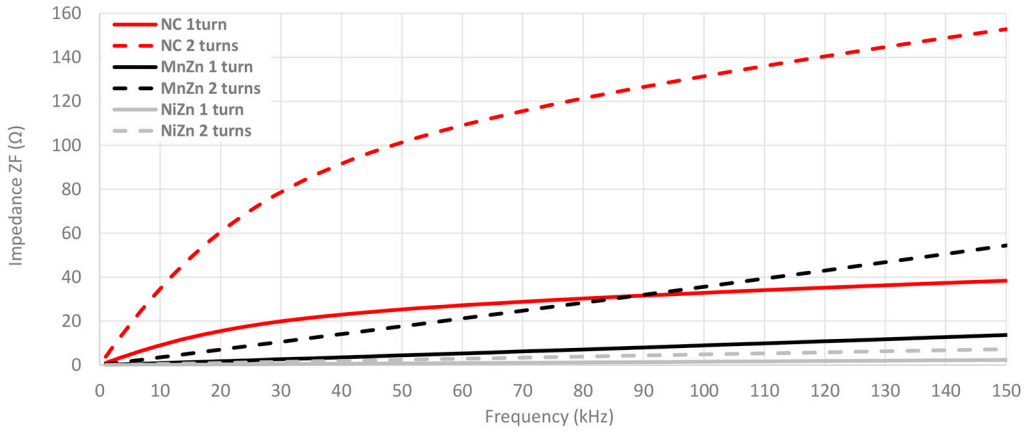

Figure 8. Impedance comparison of the three cable ferrites measured with 1 and 2 turns in the low frequency range.

Once the magnitude impedance has been analyzed, the insertion loss parameter is calculated through Equation 4 from Z_F measured of each cable ferrite, Z_A = 50 Ω and Z_B = 5 Ω. Figure 9 shows the calculated or theoretical insertion loss parameter of the three cable ferrites with one and two turns of cable winded. As illustrated in Figure 9, NC is again the composition that provide the best performance to attenuate the electromagnetic noise until 150 kHz. Moreover, all insertion loss traces are proportional to the magnitude impedance above represented. Taking 100 kHz as a reference point, NC attenuates 2.8 dB more than MnZn and 3.8 dB than NiZn cable ferrites with one turn. In the case of two turns, NC attenuation is 6.3 dB higher than MnZn and 9.9 dB than NiZn cable ferrites.

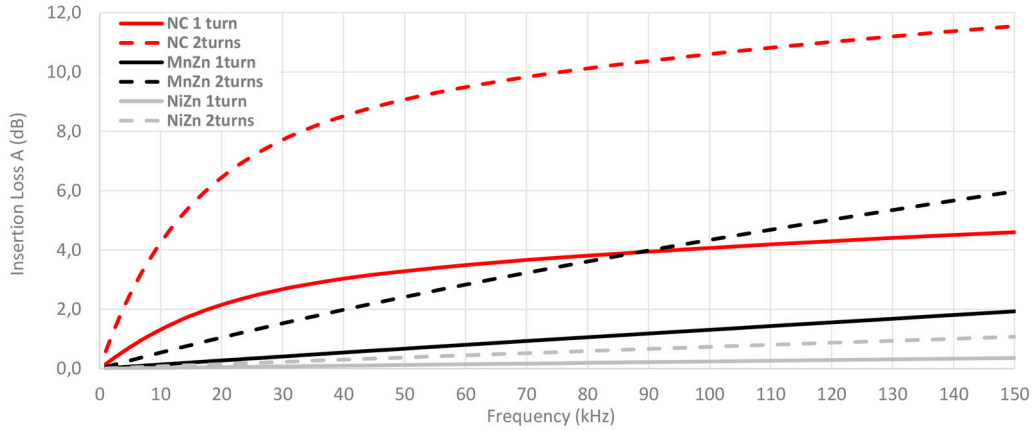

Figure 9. Theoretical insertion loss comparison depending on the material composition calculated with a 5 Ω load and winding 1 and 2 turns.

Another factor to consider is the performance of cable ferrites in systems with different impedance and thus, it could be interesting to study the insertion loss parameter by including several values of Z_A and/or Z_B in Equation 4. Consequently, Figure 10 shows a comparison among the insertion loss parameter calculated from Z_F measured of each cable ferrite with one turn, setting Z_A = 50 Ω and Z_B = 5 Ω or Z_B = 50 Ω. This chart illustrates how the higher the system output impedance in which the cable ferrite is included the lower the insertion loss that is able to provide the cable ferrite. At 100 kHz frequency point, there is a difference of 1.6 dB between the NC traces with 5 Ω and 50 Ω, 0.5 dB in the case of MnZn traces and 0.2 dB for NiZn traces.

Preprints (www.preprints.org) | NOT PEER-REVIEWED | Posted: 13 December 2017 doi:10.20944/preprints201712.0081.v1

Peer-reviewed version available at Materials 2018, 11, 174; doi:10.3390/ma11020174

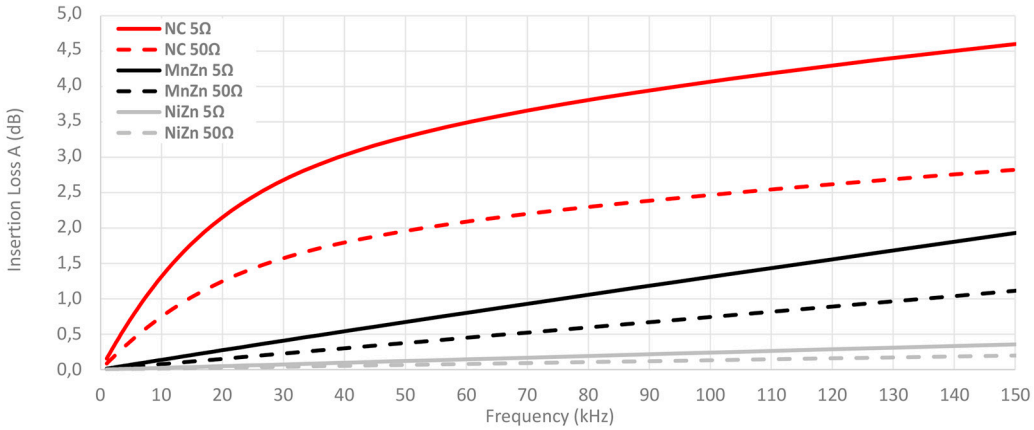

Figure 10. Theoretical insertion loss comparison depending on the material composition calculated with 5 Ω and 50 Ω loads by winding 1 turn.

This connection between the system impedance and the ability of cable ferrites to attenuate the interferences is displayed in Figure 11, where the insertion loss is calculated by setting Z_A = 50 Ω and Z_B is switched among the next values: 5 Ω, 50 Ω, 100 Ω and 1000 Ω. The material selected to analyze this connection is the NC due to it provides the best performance in this frequency range. Thereby, this graph shows that the theoretical insertion loss is much reduced when the impedance of the system is close to 1kΩ. However, if the system has an input impedance of 50 Ω and an output impedance less than 100 Ω the NC cable ferrite with one turn can provide a useful behavior.

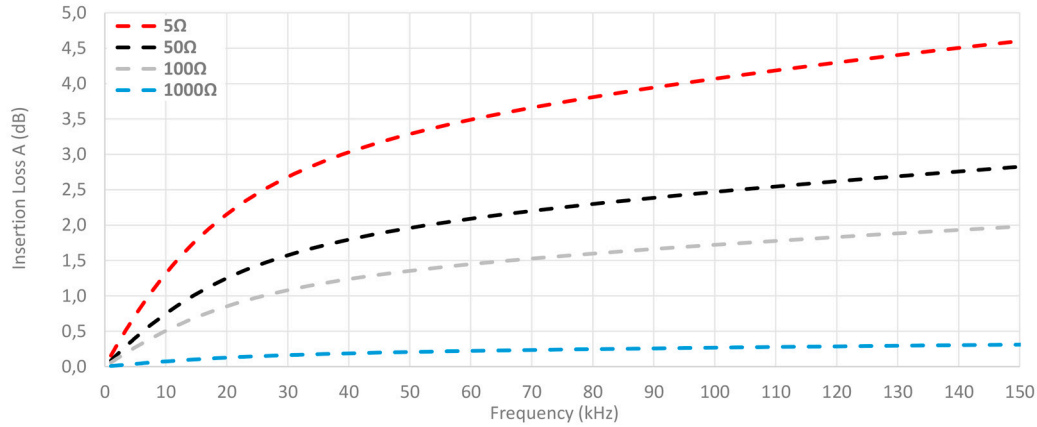

Figure 11. Theoretical insertion loss comparison depending on load calculated with 5 Ω, 50 Ω, 100 Ω and 1000 Ω loads by winding 1 turn in the NC cable ferrite.

3.2 Experimental Insertion Loss Results

The experimental insertion loss is measured by following the procedure explained in 2.3 section. Figure 12 shows an example of the measurement method used to determine the insertion loss parameter with one turn (a) and two turns (b). Experimental insertion loss is determined by subtracting to the trace 1 (yellow), which represents the reference before placing any cable ferrite in the system, one of the other three traces. Trace 2 (blue) represents the signal measured after placing the NC cable ferrite, trace 3 (purple) corresponds to MnZn and trace 4 (blue) is acquired when NiZn cable ferrite is placed. Therefore, the insertion loss of NC cable ferrite at 100 kHz is given by subtracting markers 1 and 2 represented in the table below the spectrum in (a) in the case of one turn and (b) in the case of two turns. As a result of this step, the insertion loss obtained for the NC cable ferrite is 3.486 dB with one turn and 9.993 dB when the cable ferrite is winded with two turns. Consequently, by extrapolating this method to the whole frequency range of 2-150kHz it is possible to obtain the performance of each material in terms of attenuation ratio.

Preprints (www.preprints.org) | NOT PEER-REVIEWED | Posted: 13 December 2017 doi:10.20944/preprints201712.0081.v1

Peer-reviewed version available at Materials 2018, 11, 174; doi:10.3390/ma11020174

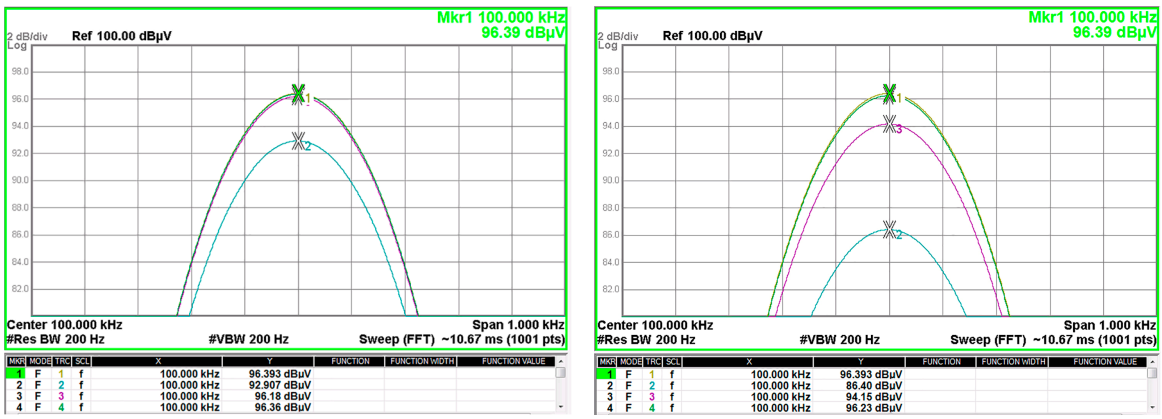

(**a**) (**b**)

Figure 12. Experimental attenuation measured with a spectrum analyzer for each cable ferrite material with a 5 Ω (Reference: trace 1 yellow, NC: trace 2 blue, MnZn: trace 3 purple, NiZn: trace 4 green): (**a**) Signal measured after placing each cable ferrite with one turn; (**b**) Signal measured after placing each cable ferrite with two turns.

A comparison between the theoretical insertion loss and the insertion loss measured with the three material cable ferrites with one turn winded is shown in Figure 13. The measured value of NC cable ferrite is 1.2 dB lower than the theoretical NC trace at 20 kHz, although, at 100 kHz this difference is reduced up to 0.6 dB. Nevertheless, in the case of MnZn and NiZn, the higher the frequency, the higher the difference between theoretical and experimental insertion loss. Hence, NC traces trend is very similar but theoretical and experimental traces of MnZn and NiZn does not follow the same trend.

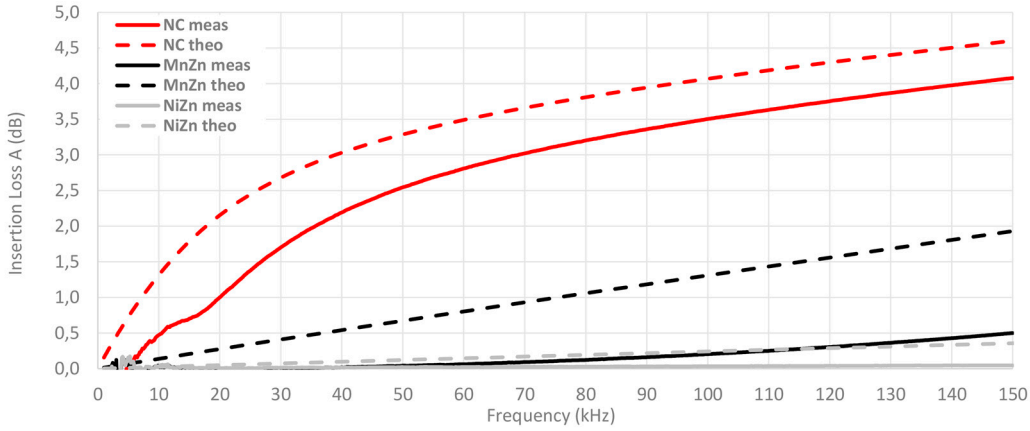

Figure 13. Experimental insertion loss comparison depending on the material composition calculated with 5 Ω and 50 Ω loads by winding 1 turn.

Figure 14 shows the same comparison that the last graph but in this case, the number of turns winded with the cable in the cable ferrite is two. It can be observed how the difference between theoretical and measured traces is lower with two turns. At 20 kHz, the NC insertion loss measured is 1.8 dB lower than theoretical value and this difference is reduced up to in 0.6 dB at 100 kHz. Thus, the relative error has been reduced taking into account that the attenuation ratio has been almost tripled (from 3.5 dB to 10.1 dB at 100 kHz in the case of measured insertion loss traces). With regard to MnZn, the trend of measured insertion loss trace has been modified and the difference with the theoretical trace has been reduced. This effect can also be observed in the NiZn traces, although to a lesser extent than NC and MnZn.

Peer-reviewed version available at Materials 2018, 11, 174; doi:10.3390/ma11020174

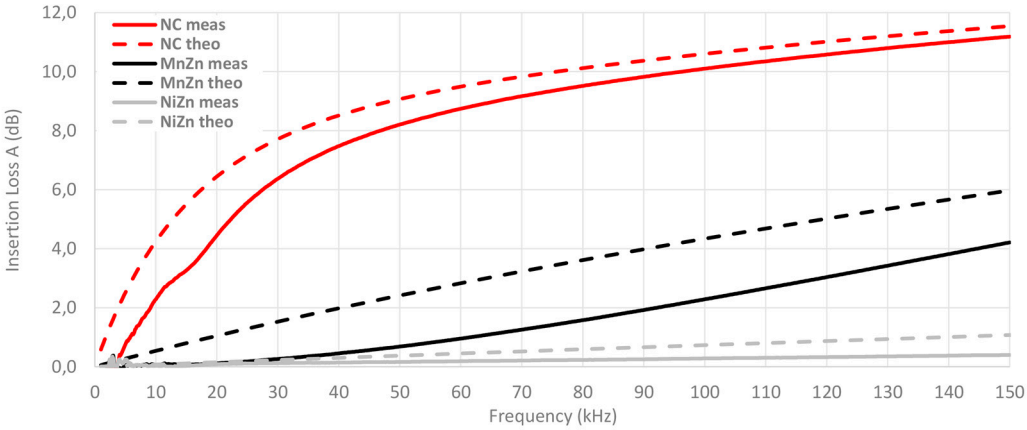

348

349 **Figure 14.** Experimental insertion loss comparison depending on the material composition calculated
350 with 5 Ω and 50 Ω loads by winding 1 turn.

351 Another point to take into account is the connection between the impedance of the system where
352 the cable ferrite is placed and the insertion loss that it is able to provide. In order to evaluate this, the
353 insertion loss of the NC cable ferrite is measured by setting Z_A = 50 Ω and modifying Z_B among the
354 next values: 5 Ω, 50 Ω, 100 Ω and 1000 Ω. Figure 15 shows this comparison combined with the
355 theoretical insertion loss traces showed in the Figure 11. According to the graph, traces that represent
356 measured insertion loss are lower than theoretical traces, although trend of both is very similar. Just
357 as theoretical NC trace, the experimental insertion loss measured showed in this graph is insignificant
358 when the system impedance is close to 1000 Ω.

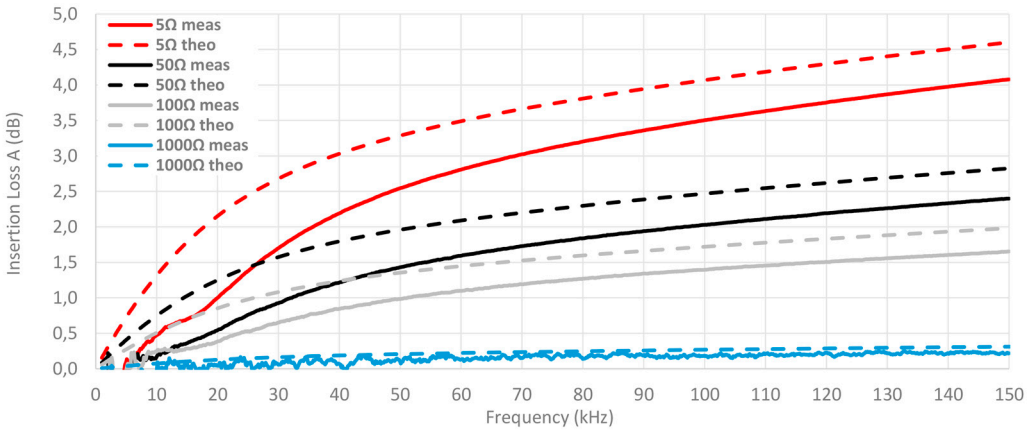

359

360 **Figure 15.** Comparison between experimental and theoretical insertion loss of NC cable ferrite
361 depending on the load by winding 1 turn.

362 Figure 16 shows the same comparison that Figure 15, but in this case, two turns are winded in
363 the NC cable ferrite. Therefore, the difference between measured and theoretical insertion loss is
364 reduced regardless of the system impedance. Moreover, it can be observed that the higher the
365 frequency, the lower the difference between theoretical and experimental insertion loss.

Peer-reviewed version available at Materials 2018, 11, 174; doi:10.3390/ma11020174

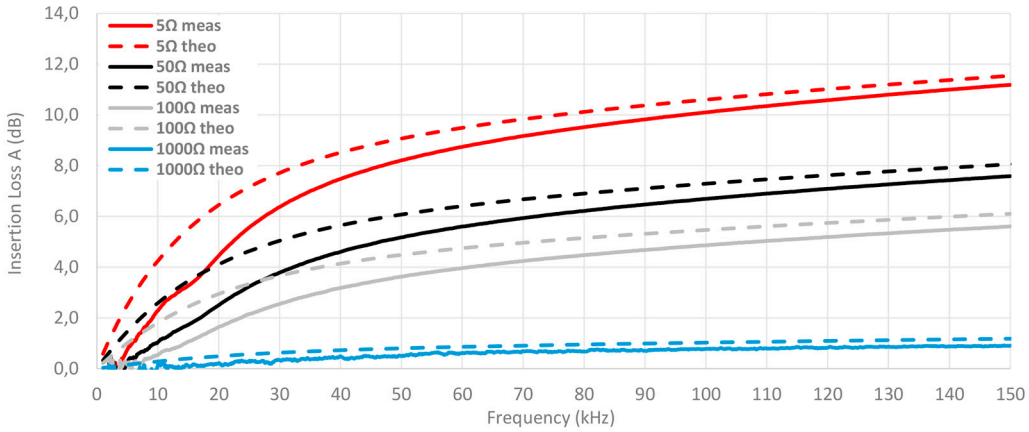

Figure 16. Comparison between experimental and theoretical insertion loss of NC cable ferrite depending on the load by winding 2 turn.

Considering that the difference between theoretical and experimental insertion loss traces is lower at high frequencies, the insertion loss has been measured with a general purpose signal generator with the aim of obtain a qualitative trend up to 1 MHz. This measurement has been carried out for the three cable ferrites with one turn and compared with the calculated insertion loss in Figure 17. Therefore, it is possible to observe that the difference between NC traces is lower at high frequency and MnZn traces match at 700 kHz. Nevertheless, the difference between NiZn traces is higher at 1 MHz.

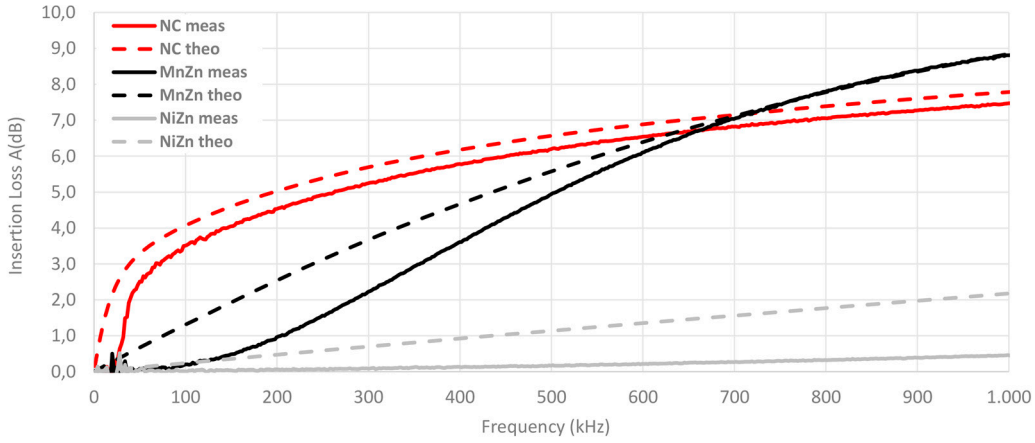

Figure 17. Comparison between experimental and theoretical insertion loss of different cable ferrites depending on the material composition by winding 1 turn at higher frequencies.

4. Conclusions

The results presented in this contribution demonstrates the suitability of cable ferrites based on nanocrystalline composition in the 2-150 kHz frequency range in comparison with others based on MnZn or NiZn. This has been verified theoretically through measuring the impedance of each cable ferrite material and calculating the insertion loss and taking into account the system impedance where the component is placed. A way of determining the attenuation ratio or insertion loss through an experimental setup has been proposed and these measurements has been matched with the theoretical insertion loss in order to check the accuracy of this technique. Thereby, the measurements performed both theoretical and experimental, indicates that NC provides greater losses at low frequencies than MnZn and NiZn as shown the relative permeability graph.

The system impedance parameter has been modified to study the performance of cable ferrites with several output impedances and the results show that the attenuation ratio is too low in systems with an impedance close to 1000 Ω. Likewise, the analysis has been done with one and two turns

around the cable ferrites in order to take into account the performance of each material when the number of turns is increased. These last measurements show that the difference between measured and calculated insertion loss is reduced. It could take place due to the inductance and resistance parts of the magnitude impedance are shifted. Thus, it can generate a change in the trend of the insertion loss measured trace. Consequently, a new line of research can be carried out from the results of this contribution, due to a setup can be designed to determine the insertion loss with the aim of evaluating cable ferrites at higher frequencies. This method could make it possible to study the accuracy of the insertion loss mathematical expression in order to know if R and X_L should be considered with a different weight in this equation.

Acknowledgments: This work was supported by the Catedra Würth-EMC, a research collaboration agreement between the University of Valencia and Würth Elektronik eiSos GmbH & Co. KG.

Author Contributions: J. Victoria and J. Torres conceived and designed the experimental measurement setup; A. Alcarria, P.A. Martinez, J. Soret and J. Martos performed the experiments; A. Suarez, R. Garcia-Olcina and P.A. Martinez analyzed the data; A. Suarez, R. Garcia-Olcina, J. Soret, J. Martos, J. Torres and J. Victoria wrote and reviewed the paper.

Conflicts of Interest: The authors declare no conflict of interest. The founding sponsors had no role in the design of the study; in the collection, analyses, or interpretation of data; in the writing of the manuscript, and in the decision to publish the results.

References

1. Bollen, M.; Olofsson, M.; Larsson, A.; Rönnberg, S.; Lundmark, M. Standards for supraharmonics (2 to 150 kHz). *IEEE Electromagnetic Compatibility Magazine* **2014**, *3*, 114-119, doi:10.1109/MEMC.2014.6798813.
2. Luszcz, J. High Frequency Harmonics Emission in Smart Grids. In *Power Quality Issues*; Zobaa, A., Eds.; InTech: Rijeka, Croatia, 2013; pp. 277-280, ISBN 978-953-51-1068-2.
3. Schöttke, S.; Meyer, J.; Schegner, P.; Bachmann, S. Emission in the frequency range of 2 kHz to 150 kHz caused by electrical vehicle charging. In Proceedings of the International Symposium on Electromagnetic Compatibility, Gothenburg, Sweden, September 2014, pp. 620-625.
4. Rönnberg, S.; Bollen, M.; Larsson, A. Emission from small scale PV-installations on the low voltage grid. In Proceedings of the International Conference on Renewable Energies and Power Quality, Córdoba, Spain, April 2014; pp. 617-621.
5. Bartak, G.F.; Abart, A. EMI of emissions in the frequency range 2 kHz-150 kHz. In Proceedings of 22nd International Conference and Exhibition on Electricity Distribution, Stockholm, Sweden, June 2013.
6. Gil-de-Castro, A.; Rönnberg, S.K.; Bollen, M.H.; Moreno-Muñoz, A.; Study on harmonic emission of domestic equipment combined with different types of lighting. *International Journal of Electrical Power & Energy Systems* **2014**, *55*, 116-127, doi:10.1016/J.IJEPES.2013.09.001.
7. Subhani, S.; Cuk, V.; Coben, J. F. G. A Literature Survey on Power Quality Disturbances in the Frequency Range of 2–150 kHz. In Proceedings of the International Conference on Renewable Energies and Power Quality, Málaga, Spain, April 2017; pp. 405-410.
8. Smolenski, R. Conducted Electromagnetic Interference (EMI) in Smart Grids. In *Power Systems*; Springer Science & Business Media: London, UK, 2012; ISBN 978-1-4471-2959-2.
9. Coenen, M.; van Roermund, A. Conducted mains test method in 2–150 kHz band. In Proceedings of the International Symposium on Electromagnetic Compatibility, Gothenburg, Sweden, September 2014, pp. 601-604.
10. Ott, H. W. *Electromagnetic Compatibility Engineering*; John Wiley & Sons: New Jersey, USA, 2009; pp. 225-234, ISBN 978-04-7050-850-3.
11. Brander, T.; Gerfer, A.; Rall, B.; Zenkner, H. *Trilogy of Magnetics: Design Guide for EMI filter design, SMP & RF circuits*, 4th ed.; Swiridoff Verlag: Künzelsau, Germany, 2010; ISBN 978-3-89929-157-5.
12. Lukovic, M. D.; Nikolic, M. V.; Blaz, N. V.; Zivanov, L. D.; Aleksic, O. S.; Lukic, L. S. Mn-Zn ferrite round cable EMI suppressor with deep grooves and a secondary short circuit for different frequency ranges. *IEEE Transactions on Magnetics* **2013**, *49*, 1172-1177, doi:10.1109/TMAG.2012.2219064.
13. Tsutaoka, T. Frequency dispersion of complex permeability in Mn–Zn and Ni–Zn spinel ferrites and their composite materials. *Journal of Applied Physics* **2003**, *93*, 2789-2796, doi:10.1063/1.1542651.

14. Herzer, G.; Vazquez, M.; Knobel, M.; Zhukov, A.; Reininger, T.; Davies, H. A.; Ll, J. S. Round table discussion: Present and future applications of nanocrystalline magnetic materials. *Journal of Magnetism and Magnetic Materials* **2005**, *294*, 252-266. doi:10.1016/J.JMMM.2005.03.042.
15. Thierry, W.; Thierry, S.; Benoît, V.; Dominique, G. Strong volume reduction of common mode choke for RFI filters with the help of nanocrystalline cores design and experiments. *Journal of Magnetism and Magnetic Materials* **2006**, *304*, 847-849, doi:10.1016/j.jmmm.2006.03.014.
16. Liu, Y.; Han, Y.; Liu, S.; Lin, F. Pulse Magnetic Properties Measurement and Characterization of Fe-Based Nanocrystalline Cores for High-Voltage Pulse Magnetics Applications. *IEEE Transactions on Power Electronics* **2015**, *30*, 6883-6896, doi:10.1109/TPEL.2014.2386916.
17. Gony, B.; Camus, S.; Hill, J.; Pottier, F. A New Generation of Nanocrystalline Magnetic Cores with Very Low Magnetic Losses. In Proceedings of the International Conference for Power Electronics, Intelligent Motion, Renewable Energy and Energy Management, Nuremberg, Germany, May 2016; pp. 1-7.
18. Goldman, A. *Modern ferrite technology*, 2nd ed.; Springer Science & Business Media: Pittsburgh, PA, USA, 2006; ISBN 978-0-387-28151-3.
19. Suarez, A.; Victoria, J.; Alcarria, A.; Torres, J. Characterization of electromagnetic noise suppression sheet for aerospace applications. In Proceedings of the ESA Workshop on Aerospace EMC, Valencia, Spain, May 2016; pp. 1-6.
20. Sharma, A.; Rahman, N.; Obol, M.; Afsar, M. Precise characterization and design of composite absorbers for wideband microwave applications. In Proceedings of European Microwave Conference, Paris, France, September 2010; pp. 160-163.
21. Keysight E5061B-3L3/3L4/3L5 LF-RF Network Analyzer with Option 005 Impedance Analysis Function. Available online: http://literature.cdn.keysight.com/litweb/pdf/5990-7033EN.pdf (accessed on 22 November 2017).